47th European Rotorcraft Forum

PARTICLE TRACKING ANALYSIS OF A ROTOR IN GROUND EFFECT

Federico Rovere, [1] George N. Barakos, [2] René Steijl [3]
CFD Laboratory, School of Engineering, University of Glasgow, G12 8QQ, U.K.
www.gla.ac.uk/cfd

Abstract

In the present work, computational fluid dynamics (CFD) is used to predict the behavior of ground particles, uplifted by a two-bladed rotor. The paper focuses on defining a safety area where the presence of particles can be considered as negligible, and compare this area with other distance based criteria. Using data of three different aircraft, scaling factors have been used to take into account the different size of the small-rotor studied and real case scenarios. The results show how heavier helicopters may generate the most dangerous situations, in terms of presence of particles in a delimited area.

Nomenclature

Latin

a	Speed of sound, m/s
B	Ballistic Coefficient, kg/m^2
c	Blade chord, m
C_Q	Rotor torque coefficient,
C_T	Rotor thust coefficient,
D	Rotor diameter, m
d_p	Particle diameter, m
FoM	Figure of merit, FoM
g	Gravitational acceleration, m/s^2
M	Mach number, $M = V_{tip}c/a_\infty$
N_b	Number of blades
Q	Rotor torque, $N \cdot m$
Re	Reynolds number, $Re = V_{tip}c/\upsilon_\infty$
S_{rotor}	Rotor disk area, m^2
T	Rotor thrust, N
r	Radial coordinate along blade span, m
R	Rotor radius, m
U	Velocity x-component, m/s
$u*$	Friction velocity, m/s
V	Velocity y-component, m/s
V_{rad}	Velocity radial component, $V_{rad} = Ucos(\Psi) + V sin(\Psi)$, m/s

Greek

λ_i	Hover induced velocity, $\lambda_i = \sqrt{\frac{C_t}{2}}$
Ψ	Local azimuth angle, deg
ρ	Density, kg/m^3
τ_w	Wall shear stress, kg/ms^2
θ	Collective pitch at three-quarter radius, deg
υ	Kinematic viscosity, m^2/s
Ω	Rotor angular velocity, rad/s

Super and subscripts

∞	Freestream value
fs	Full-scale

---

[1] PhD Student - federico.rovere@glasgow.ac.uk
[2] Professor - george.barakos@glasgow.ac.uk - corresponding author
[3] Senior Lecturer - rene.steijl@glasgow.ac.uk

p	Particle
ss	Small-scale
tip	Blade tip value

Acronyms

CFD	Computational Fluid Dynamics
DVE	Degraded Visual Environment
IGE	In Ground Effect
$MTOW$	Maximum TakeOff Weight
$MUSCL$	Monotone Upstream Centred Schemes for Conservation Laws
OGE	Out of Ground Effect
PIV	Particle Image Velocimetry

1. INTRODUCTION

The interaction between the lifting rotor wake and a sediment bed may cause the uplift of particles, including sand, dust, snow and even small rocks. This phenomenon is called brownout, in case of sand and dust, and whiteout in presence of water droplets and snow. Both phenomena may afflict helicopters in hover and taxiing. The entrained particles are advected by the air flow and may collide with the aircraft structure. Their impact can generate erosion and damages to the structure, and also, they can be ingested by the aircraft engine leading to performance reductions. Despite the importance of erosion effects, the most dangerous consequence of Brown and Whiteout is the degradation of the pilot's visual environment. At certain flight and environmental conditions, the entrained particles may generate a cloud all around the aircraft. In these conditions of Degraded Visual Environment (DVE), the cloud causes a reduction of the pilot visibility and increases the risk of impact with a ground object. Brownout is one of the most dangerous scenario that a helicopter may occur during an IGE operations. In recent years, efforts have been made to help pilots in these situations, developing sensors and advanced cockpit displays. Dynamic rollover and collisions with objects are common accidents due to the lack of visibility [1]. US Air force lost 30 special operation aircraft and 60 crew members lost their lives during landing in desert environments since 1990 [2]. In the same report authors specify that brownout cost to US services is estimated at $100M/yr. Other NATO members experienced similar statistics. UK had 24 brownout mishaps in the period 2005-2009. The German defense force had more than 30 accidents due to dust and snow [2]. The occurrence of brownout is the most common cause of human factor mishaps during military operations [3]. Rotor wakes have a key role in the brownout cloud development, furthermore they can be a source of risks for ground personnel, equipment and landscape due to the forces generated by high outflow velocities. Risks related to wake encounters and the FAA safety separation criteria are widely discussed in [4]. For these reasons, rotor wakes IGE have been studied in depth in past years following different approaches, from full-scale aircraft [5], to small-scale isolated rotors [6, 7]. In the first case, during experiments, the operational scenario it is fully replicated using full-scale aircraft in different scenarios, taking measurements during aircraft flight. [8] [5]. In general, however, measurement techniques used in full-scale experiments, lack high resolution, and cannot provide a detailed view of the phenomena involved. On the other hand, small-scaled studies can be performed in a laboratory, within a controlled environment. Particle Imagine Velocimetry (PIV) and other high-resolution measuring techniques are widely used during these studies. However, due to the limited size of the rotors, Reynolds number and Mach number are lower with respect to the full-scale case, leading to some differences in the flowfield behavior.

In the present work, computational fluid dynamics (CFD) has been used to predict the flowfield around a micro two-bladed rotor operating IGE. The test case simulated was experimentally investigated at the University of Maryland by Lee et al. [6]. Experimental results have been used to full validate CFD results in terms of rotor performance and outflow velocities. The full test case validation is contained in previous works [9] [10]. The outflows produced were used to evaluate particle uplift and particle tracking. To obtain realistic full-scale scenarios, a scaling factor has been applied to flowfield velocities. Three different aircraft data have been used, categorized in terms of weight. Considering the uplift area of particles, and their path it is possible to define safe zones where it was possible to consider the presence of the particles as negligible. Existing safety separation criteria can then be tested. A possible separation distance is suggested by FAA for wake encounters [11] [4]. In that case, a distance of 3 rotor diameters is suggested to allow the dissipation of the wake generated by a rotor in hover or taxiing. Investigations are conducted to verify if the same distance can be considered safe for the presence of particles in the area that can spoil the pilot view of a near aircraft or hit people operating inside the 3 rotor diameters area. All CFD simulations have been performed using the HMB3 (Helicopter Multi-Block) CFD solver of Glasgow University.

2. NUMERICAL MODELS

2.1 CFD SOLVER

HMB3 (Helicopter Multi-Block) [12, 13] is the solver used for all CFD simulations in this work. It solves the Unsteady Reynolds Averaged Navier-Stokes equations (URANS) in integral form with ALE formulation (Arbitrary Lagrangian Eulerian) for time-dependent domains (moving boundaries). URANS equations are discretized using a cell-centered finite volume approach on a multiblock structured grid. HMB3 uses the Osher [14] and

Roe [15] approximate Riemann solvers to evaluate the convective fluxes. The viscous terms are discretized using second order central differencing. Third order accuracy in space is provided by the Monotone Upstream Centred Schemes for Conservation Laws (MUSCL) [16]. To avoid non-physical spurious oscillations where large gradients are involved in computations (like shockwaves), HMB3 uses a modified form of the Albada limiter [17]. An implicit dual time stepping method is employed to perform the temporal integration. Oversets grids (used in this work) [18] and sliding plane [19] methods are available in HMB3 to allow for the relative motion between mesh components, representing ground and rotor blade. Various turbulence models are available in HMB3, including one- equation, two-equation, three and four equations turbulent models. Large-eddy Simulation (LES), Detached- Eddy Simulation (DES) and Delay-Detached-Eddy Simulation (DDES) can also be used with HMB3. For this study two different turbulence model have been used: k ω and k ω SST [20], furthermore due to the low Reynolds numbers of the test cases a small number of laminar simulations were also performed.

2.2 SCALING THE FLOWFIELD

Analyzing flowfield velocities generated by a small-scale rotor is not possible for safety purposes. They are simply too low and harmless to generate any kind of hazards. For this reason, two scaling factors have been applied to flowfield velocities. The first scaling is necessary to obtain values comparable to full scale rotor wake velocities. The second is used to take into account the difference in thrust coefficient of the small- and full-scale scenario. The blade tip velocity has been used as first scaling factor, which is listed in table 1 for full scale rotors. For the second scaling factor the hover induced velocity has been considered. In general, the hover induced velocity is a common reference value for outflow velocities. When it is scaled with V_{TIP}, the hover induced velocity is expressed as $\lambda_I = \surd C_T/2$. The scaled rotor thrust coefficient obtained by the simulation of the micro rotor is $C_T^{ss} = 0.03$, while the C_T^{fs} can be obtained by the aircraft data. Assuming the aircraft in hover flight, and thrust equal to the weight, which is considered the maximum at take off. W_{MTOW} , V_{tip}, and S_{rotor} are specified in table 1, while for the acceleration of gravity and for the air density the following values have been assumed: g=9.81m/s^2 and ρ_{air}= 1.225kg/m^3.

(1) $$C_T^{fs} = \frac{2W_{MTOW}}{\rho_{air}V_{tip}^2 S_{roto}}$$

It is possible, taking into account the effect of the different thrust coefficient to scale the velocities using the ratio of hover induced velocity between full-scale and small-scale cases. The scaling factor obtained is $\sqrt{\frac{C_T^{fs}}{C_T^{ss}}}$. This way, it is possible to estimate the outflow velocities generated by a full-scale rotor operating at the same high values of thrust coefficient of the scaled rotor. The final scaling factor increase the value of the velocities involved in the simulations, due to the stronger influence of the higher rotor tip velocity. It is important to say that this kind of scaling cannot fully represent the complexity of the phenomena involved. This approach does not take into account the different Reynolds numbers that are involved in full- and small-scale rotors, which may deeply change the wake and its development in time.

2.3 PARTICLE TRACKING

Brownout and whiteout are due to the presence in the flowfield of particles. The former involves sand, and the latter snow. However, in general, all kinds of particles can be involved such as rain, ice and even small rocks. To properly simulate the behavior of them in the flowfield it is necessary to model their motion. There are basically two approaches for the numerical simulation of dispersed phases, and they can be categorized into Lagrangian tracking or Eulerian modelling approaches. In the Lagrangian approach, the particles (or parcels of particles) are tracked through the field. For methods that involve this approach the motion of the particles is tracked solving the Newton's second law. Important works in Lagrangian frame of reference are [21] [22]. In the case of Eulerian methods, the properties of the particles are assumed to be continuous within the field. Thus, differential conservation equations are written, discretized, and the solution of these gives the properties of the cloud (size, number of particles involved, density etc.). Eulerian formulation can be based on number of particle density, [23], or on solid mass particle density [24]. A particle tracking tool has been developed for this work. A pick-up model, based on threshold velocity, has been used to analyze the particle uplift from the ground. Using this information, it was possible to seed properly the ground and track the particles in the flowfield, using a Lagrangian frame of reference.

2.3.1 PARTICLE UPLIFT

When the wake reaches the ground and interacts with the loose sediment, particles can be uplifted. The Bangold model (see [25, 26]) has been used to simulate brownout in several works. It has been developed within the sediment community to simulate the pick-up of particles in river flows. In 2000 Shao et al. [27] proposed a simple formulation for particles pick-up, based on Bangold model, that has been used in this work. It is a threshold model, based on the wall friction velocity $u_* = \sqrt{\frac{\tau_w}{\rho}}$. The threshold value is function of particle and fluid proprieties and on the gravity. It is computed as:

(2) $$u_t^* = \sqrt{A(\frac{\rho_p}{\rho_{air}} g d_p + \frac{\beta}{\rho_{air} d_p})}$$

where u_t^* is the threshold velocity, while A and β are coefficients: A=0.0123, β=0.0003 kg/s^2 . The particle values, used in this work, are listed in Table 2, while for air density and gravity the following values have been used ρ_{air} = 1.225 kg/m^3 and g = 9.81m/s^2. When u_* > u_t^* the particle is uplifted, and it is entrained the flowfield. Another cause of particle uplift is "splash entrainment". Anytime an entrained particle hits the ground, it may have sufficiently high energy to launch more particles.

The kinetic energy gained by the hit particles can overcome the cohesive forces and lead uplift. This phenomenon has not been taken into account in the present simulations, but it is described in [28] and [27].

2.3.2 PARTICLE TRACKING METHOD

For particle tracking, a simulation tool has been used. The particles are driven by the flowfield velocities and their positions in time are obtained by integrating their equations of motion. The integration method used is a forth order Runge-Kutta, and the equation for particle tracking acceleration is.

$$\boldsymbol{a}_p = \frac{0.5\rho_{air}(\boldsymbol{u}-\boldsymbol{u}_p)||(\boldsymbol{u}-\boldsymbol{u}_p)||}{B} - \boldsymbol{g} \tag{3}$$

Where $\boldsymbol{a}_p$ is the acceleration of the particle, $\boldsymbol{u}_p$ is its velocity, $\boldsymbol{u}$ is the velocity of the flowfield in the position of the particle and B the ballistic coefficient, B=$m_p/S_{rotor}C_{d.}$ Here m_p is the particle mass, $S_p = \pi d^2/4$ is the particle frontal area (particles are assumed spherical) and C_D the particle drag coefficient, and finally **g** is acceleration of gravity. The particle proprieties used in this work are listed in table 2, they reflect the size and the density of particles used to simulate brownout in experimental and computational works[29][30][31]. Particle tracking computations have been performed solving the described equations in dimensionless form. The reference values for length was c, rotor aerodynamic chord. For density was free-stream density ρ_∞ , and for velocity was rotor tip velocity V_{tip}.

3. COMPUTATIONS AND SAFETY CONSIDERATIONS

Previous works show in detail the full validation of this test case in OGE [10] and IGE [9]. IGE configuration the rotor was modelled using two overset grids, and the ground was modelled imposing no-slip conditions. The full rotor domain was computed as unsteady. The unsteady time step was changed during the simulation, starting with a big timestep which was gradually reduced reaching 0.5deg/timestep for the last revolutions performed. Simulations performed in total 5 full revolutions. The mesh has been refined near the ground and the rotor to accurately resolve the wake features. Three different rotor height above the ground configuration were tested: h/R=0.5, h/R=1 and h/R=1.5, all of them with collective θ = 12deg. Full comparison of performance and outflows results can be found in [10] and [9]. Uplift of particles is shown in figure 1. The computed shear stress on the ground of the domain allowed to calculate the particle velocity uplift threshold. In general results show that the peak of the uplift ratio u^*/u_t^* is in proximity of 1 R distance from the rotor, and the area of uplift particles for the cases considered is at least between 1R and 2R. Heavier helicopters produce stronger outflow, which may extend the uplift area up to 3R. The rotor distance from the ground have a key role in defining the area where particles may be uplifted. Results show that when the rotor operate at h/R=0.5, the particles can be uplifted up to a 3 rotor radius distance, while for higher rotor altitude the uplift area can be delimited around 2R. In figure 2 are shown the results for particle tracking. Seeding points have been released in proximity of the ground, between 1 and 2R, as result of uplift threshold model analysis. A new particle is released in the flowfield form the ground every 5deg. The full simulation involves 100 revolutions (about 30 seconds for a full-scale rotorcraft). Due to the high computational cost of the CFD simulation, the last revolution performed has been considered periodic, and it has been repeated for the full duration of the particle tracking. When the rotor is operating at h/R=1, the particles are uplifted by the flowfield, and then move away from the rotor, following the radial direction. Particles are driven by the outflow that pushes them away from the rotor. However, depending on the strength of the outflow they reach different positions. Heavy weight helicopters have a stronger outflow, and in this case, particles can reach a maximum radial distance of 8.5R, and a maximum height above the ground of 1R. Once the particles reach the maximum altitude value, they fall again on the ground. Lighter weight helicopter cases show lower values for maximum h/R and r/R, however particles go further the 3D separation criteria for wake encounters. A similar path is followed in the case of h/R=1.5, where the particles reach a maximum height of h/R=1.5 for the heavy weight aircraft case. As for the previous case, the maximum height is reached at r/R=6, however the flowfield seems weaker with respect to the previous case, particles reach a maximum radial distance of 8R, in the most dangerous scenario. On the other hand, when the helicopter is operating at h/R=0.5 particles show a different behavior. Initially particles are uplifted from the ground, then two main branches spread, following different paths. Some of them, are reingested by the rotor, reaching the highest distance from the ground. These particles can be dangerous for the crew and the aircraft. The rest of the particles keep following the radial direction far from the rotor, and fall again on the ground at distance around 6.5R for the heavy scale helicopter. Particles that move away from the rotor can be dangerous for ground personnel and equipment, while the recirculation of the particles creates risks for the helicopter and the crew itself. During the re-ingesting phase particles can hit blades and fuselage and they create the cloud that degrades the visual of the pilot, creating a dangerous DVE condition. The DVE condition is clearer in figure 3. Clouds density plots can only be relative compared, only few positions of the ground have been seeded with particles. In a real brownout scenario, particles can be uplifted from all over the ground where the outflow is strong enough, and their realizing time would be shorter than what used in these simulations. All of this will lead to higher dust density concentration. Comparing obtained results, it is clear that the cloud generated in the case of h/R=0.5 is more severe than the other two cases, due to reingestion of particles, in this case the visibility of the pilot is limited by the high amount of particles in proximity of the rotor disk. On the other hand, when the rotor is operating at h/R=1.0 and h/R=1.5 the higher values of cloud density are confined near the ground in the proximity the rotor disk. In this scenario, the pilot can have a good visibility in the nearby area of the rotor (3 rotor radius diameter), however after 3R distance the cloud starts to propagate reaching up to 8R. This scenario may generate dangerous situations for other aircraft that are operating in the same area of the rotor, spoiling other pilots' visibility or damaging aircraft structures and equipment. Results show that after 100 revolutions particles paths are closed. As previously described, some particle fall again on the ground, while other are reingested by the rotor. In both cases, however, after this period the cloud stops spreading, reaching its maximum distance.

4. CONCLUSION AND FUTURE STEPS

Particle tracking results show that particles can reach large distances away from the rotor, exceed the limit of 3D. In general, it seems that the FAA limit for wake encounters cannot guarantee safety in presence of particles on the ground. It is also clear that to define a particle free zone , it is necessary to take into account the rotor operating conditions due to the strong influence of the disk loading and in general of the size of the aircraft on the particle paths. Particle paths are also strongly influenced by the position of the rotor with respect to the ground. In this work, to obtain full-scale particle paths, scaling factors are applied to a small-scale rotor, however, the full physics of the brownout cannot be simulated in this way, due to the several factors. In general, the Reynolds number that is involved in the small and the full-scale scenario is dissimilar, leading to differences in the uplift phenomena and to a different evolution of the brownout cloud. This study can be a starting point for evaluating safe operational zones around a helicopter. A future step will involve different test case, with a rotor geometry more similar to realistic full-scale rotors and higher Reynolds number, to obtain results closer to real operational scenario. Results will be compared with distance safety regulations like the 3 rotor diameters separation distance for wake encounters suggested in the Manual of Air Traffic Service described previously. [11] [4]. Another future step of this research is to implement a bombardment model in the particle tracking tool and analyze its influence in the cloud density development.

ACKNOWLEDGMENTS

This project has received funding from the European Union's H2020 research and innovation programme under the Marie Sktodowska-Curie grant agreement No 721920

References

[1] D'Andrea, A. and Scorcelletti, F., "Enhanced numerical simulations of helicopter landing maneuvers in brownout conditions," *American Helicopter Society International 66th Annual Forum Proceedings, Phoenix, AZ* , 2010.

[2] Taskgroup, R., "Rotary-wing brownout mitigation: technologies and training," *Tech. Rep. RTO-TR-HFM-162, NATO Sci. Technol. Org.*, 2010.

[3] Mapes, P., Kent, R., and Wood, R., "DoD helicopter mishaps FY85-05: findings and recommendations," *US Air Force*, 2008.

[4] Garcia-Dorado, I., Aliaga, D. G., Bhalachandran, S., Schmid, P., and Niyogi, D., "Fast Weather Simulation for Inverse Procedural Design of 3D Urban Models," *ACM Transactions on Graphics (TOG)*, Vol. 36, No. 2, 2017, pp. 21.

[5] Silva, M. and Riser, R., "CH-47D tandem rotor outwash survey," *AHS 67th Annual Forum,Virginia Beach, Virginia, USA,*, 2011, p. 221.

[6] Lee, T. E., Leishman, J. G., and Ramasamy, M., "Fluid dynamics of interacting blade tip vortices with a ground plane," *Journal of the American Helicopter Society* , Vol. 55, No. 2, 2010, pp. 22005–22005.

[7] Milluzzo III, J. I. and Leishman, J. G., "Vortical sheet behavior in the wake of a rotor in ground effect," *AIAA Journal*, Vol. 55, No. 1, 2016, pp. 24.

[8] Wong, O. D. and Tanner, P. E., "Photogrammet- ric measurements of an EH-60L brownout cloud," 2010.

[9] Rovere, F., Barakos, G. N., and Steijl, R., "Brownout Simulations of Model-Rotors In Ground Effect," *MATEC Web of Conferences*, Vol. 314, 2020.

[10] Rovere, F., Barakos, G., and Steijl, R., "CFD validation of a micro-rotor in grond effect," *45th European Rotorcraft Forum, Warsaw*, No. 81, CFAS, 2019.

[11] CAA, "CAP 490: Manual of Air Traffic Services Part 1," 2015.

[12] Steijl, R., Barakos, G., and Badcock, K., "A framework for CFD analysis of helicopter rotors in hover and forward flight," *International journal for numerical methods in fluids*, Vol. 51, No. 8, 2006, pp. 819–847.

[13] Lawson, S., Woodgate, M., Steijl, R., and Barakos, G., "High performance computing for challeng- ing problems in computational fluid dynamics," *Progress in Aerospace Sciences*, Vol. 52, 2012, pp. 19–29.

[14] Osher, S. and Chakravarthy, S., "Upwind schemes and boundary conditions with applications to Euler equations in general geometries," *Journal of Com-*

putational Physics, Vol. 50, No. 3, 1983, pp. 447–481.

[15] Roe, P. L., “Approximate Riemann solvers, parameter vectors, and difference schemes,” *Journal of computational physics*, Vol. 43, No. 2, 1981, pp. 357–372.

[16] Van Leer, B., “Towards the ultimate conserva- tive difference scheme. V. A second-order sequel to Godunov’s method,” *Journal of computational Physics*, Vol. 32, No. 1, 1979, pp. 101–136.

[17] Van Albada, G., Van Leer, B., and Roberts, W., “A comparative study of computational meth- ods in cosmic gas dynamics,” *Upwind and High-Resolution Schemes*, Springer, 1997, pp. 95–103.

[18] Jarkowski, M., Woodgate, M., Barakos, G., and Rokicki, J., “Towards consistent hybrid overset mesh methods for rotorcraft CFD,” *International Journal for Numerical Methods in Fluids*, Vol. 74, No. 8, 2014, pp. 543–576.

[19] Steijl, R. and Barakos, G., “Sliding mesh algorithm for CFD analysis of helicopter rotor–fuselage aerodynamics,” *International journal for numerical methods in fluids*, Vol. 58, No. 5, 2008, pp. 527–549.

[20] Menter, F. R., “Two-equation eddy-viscosity turbulence models for engineering applications,” *AIAA journal*, Vol. 32, No. 8, 1994, pp. 1598–1605.

[21] Alfred, J., Celi, R., and Leishman, J. G., “Flight Path Optimization for Brownout Mitigation Using a High-Fidelity Simulation Model,” *Journal of the American Helicopter Society*, Vol. 62, No. 3, 2017, pp. 1–15.

[22] Wachspress, D., Whitehouse, G., Keller, J., Yu, K., Gilmore, P., Dorsett, M., and McClure, K., “A high fidelity brownout model for real-time flight simulations and trainers,” Vol. 1, 2009, pp. 278–301.

[23] Phillips, C., Kim, H. W., and Brown, R. E., “The flow physics of helicopter brownout,” *66th American Helicopter Society Forum: Rising to New Heights in Vertical Lift Technology* , 2010.

[24] Ghosh, S., Lohry, M. W., and Rajagopalan, R. G., “Rotor configurational effect on rotorcraft brownout,” *28th AIAA Applied Aerodynamics Conference*, 2010, p. 4238.

[25] Bagnold, R., “The physics of blown sand and desert dunes,” *William Morrow & Co., New York* , 1941.

[26] Greeley, R. and Iversen, J. D., *Wind as a geological process: on Earth, Mars, Venus and Titan*, Vol. 4, CUP Archive, 1987.

[27] Shao, Y. and Lu, H., “A simple expression for wind erosion threshold friction velocity,” *Journal of Geophysical Research: Atmospheres*, Vol. 105, No. D17, 2000, pp. 22437–22443.

[28] Shao, Y. and Li, A., “Numerical Modelling of Saltation in the Atmospheric Surface Layer,” *Boundary-Layer Meteorology* , Vol. 91, No. 2, May 1999, pp. 199–225.

[29] Syal, M., Govindarajan, B., and Leishman, J., “Mesoscale sediment tracking methodology to analyze brownout cloud developments,” *66th An- nual Forum of the American Helicopter Society, Phoenix, AZ* , 2010, pp. 11–13.

[30] Kutz, B., Gnther, T., Rumpf, A., and Kuhn, A., “Numerical examination of a model rotor in brownout conditions,” Vol. 4, 2014, pp. 2450–2461, cited By 9.

[31] Tanner, P. E., “Photogrammetric characterization of a brownout cloud,” *67th Annual Forum of the American Helicopter Society, Virginia Beach, VA*, 2011.

[32] “Vertipedia,” `https://vertipedia.vtol.org/`, Accessed: 23-09-2019.

Category	MTOW (kg)	R (m)	V_{tip} (m/s)	C_T
Light	3000	5.5	220	0.009
Medium	8000	8.1	216	0.015
Heavy	11000	8.1	220	0.0176

Table 1: Helicopters technical data [32]

$\rho_p (kg/m^3)$	$d_p\ (\mu m)$	C_D	B	u_t^*
2650	9	1.048	0.03	0.58

Table 2: Properties of particles used in this work.

h/R	θ_{75}	C_T	Re_{tip}	M_{tip}
0.5	12deg	0.035	35000	0.08
1.0	12deg	0.03	35000	0.08
1.5	12deg	0.028	35000	0.08

Table 3: Small scale rotor data

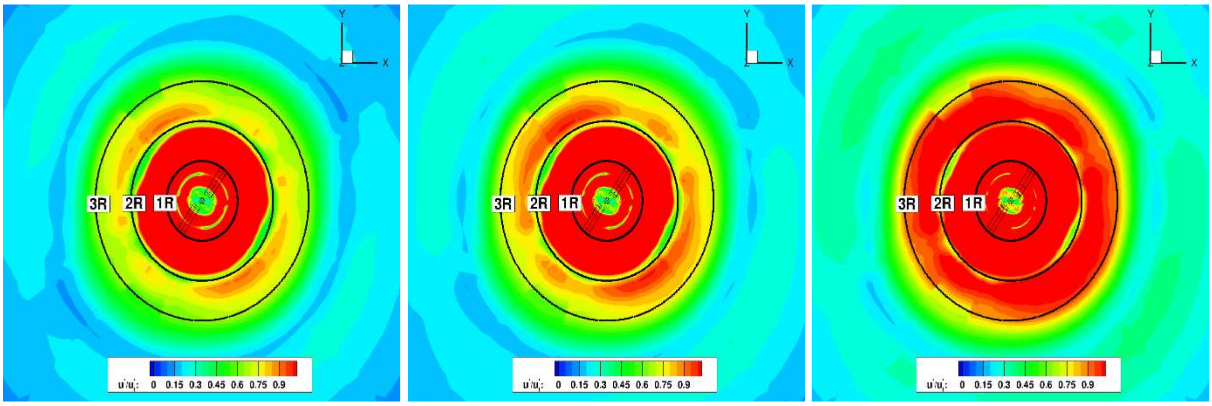

(a) Uplift for h/R=0.5, Light scale helicopter (b) Uplift for h/R=0.5, Medium scale helicopter (c) Uplift for h/R=0.5, Heavy scale helicopter

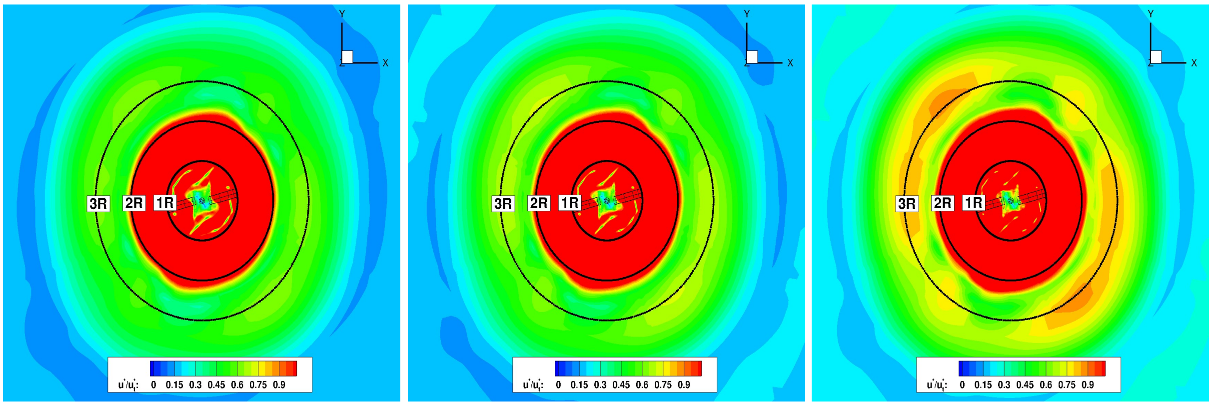

(d) Uplift for h/R=1, Light scale helicopter (e) Uplift for h/R=1, Medium scale helicopter (f) Uplift for h/R=1, Heavy scale helicopter

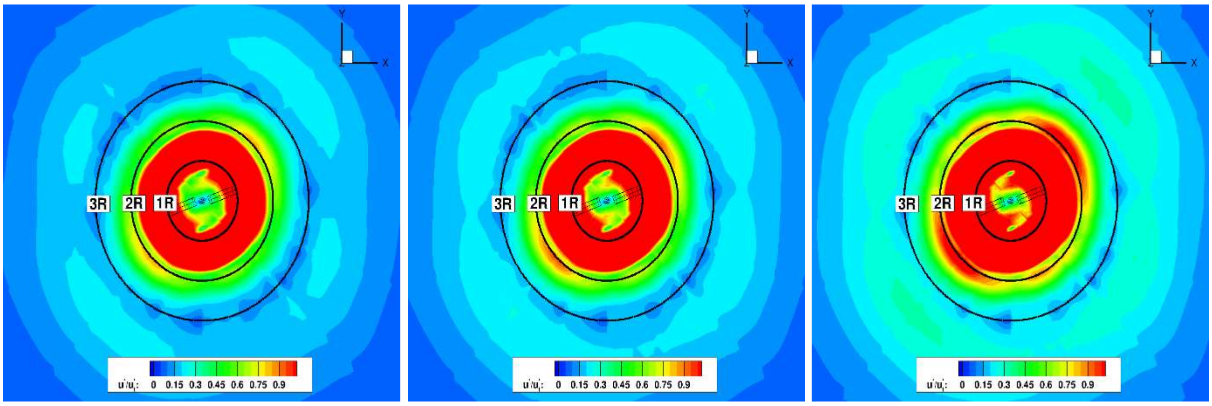

(g) Uplift for h/R=1.5, Light scale helicopter (h) Uplift for h/R=1.5, Medium scale helicopter (i) Uplift for h/R=1.5, Heavy scale helicopter

Figure 1: Uplift results for rotor at different heights above the ground and different scaling factors. All operational conditions of the small scaled rotor are listed in tab 3.

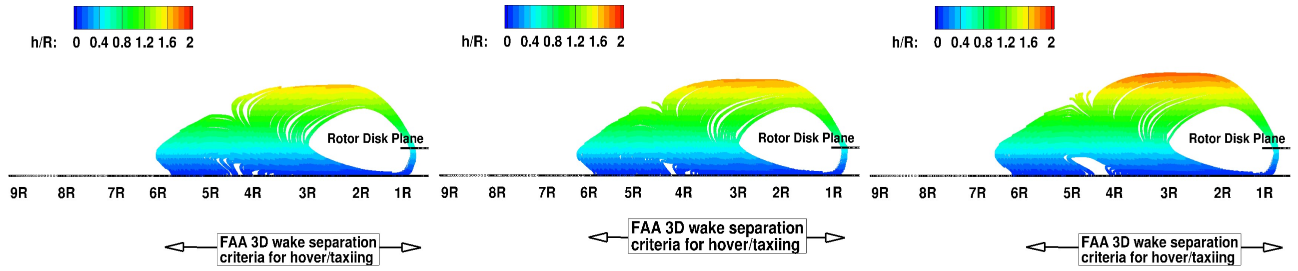

(a) Particle paths for h/R=0.5, Light scale helicopter (b) Particle paths for h/R=0.5, Medium scale helicopter (c) Particle paths for h/R=0.5, Heavy scale helicopter

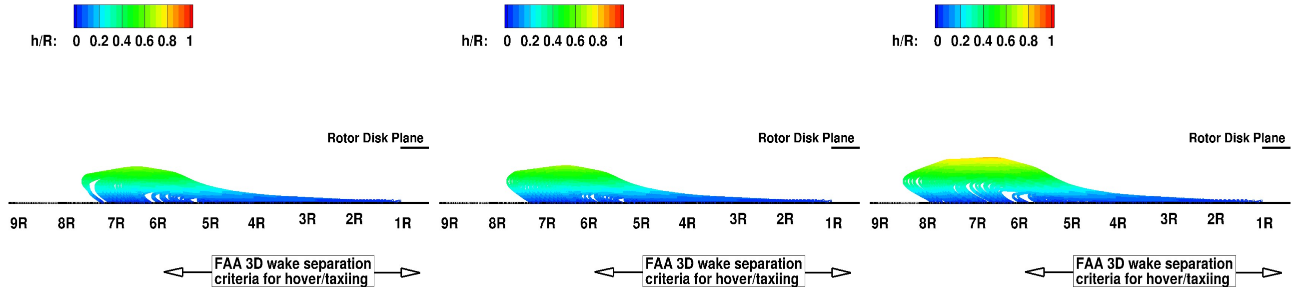

(d) Particle paths for h/R=1, Light scale helicopter (e) Particle paths for h/R=1, Medium scale helicopter (f) Particle paths for h/R=1, Heavy scale helicopter

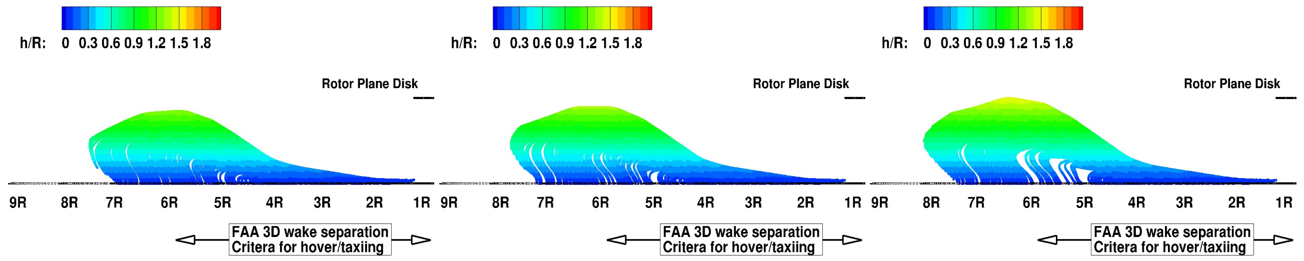

(g) Particle paths for h/R=1.5, Light scale helicopter (h) Particle paths for h/R=1.5, Medium scale helicopter (i) Particle paths for h/R=1.5, Heavy scale helicopter

Figure 2: Particle paths for rotor at different heights above the ground and different scaling factors. All operational conditions of the small scaled rotor are listed in tab 3.

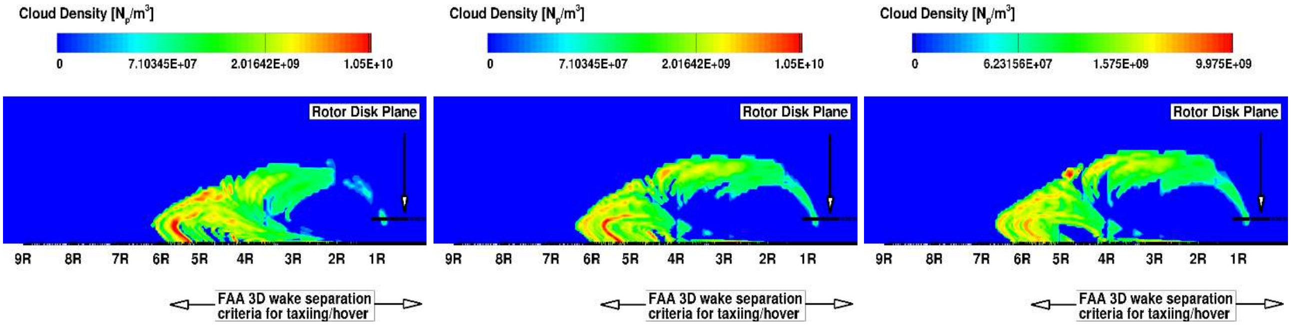

(a) Cloud density, h/R=0.5, Light scale helicopter (b) Cloud density, h/R=0.5, Medium scale helicopter (c) Cloud density, h/R=0.5, Heavy scale helicopter

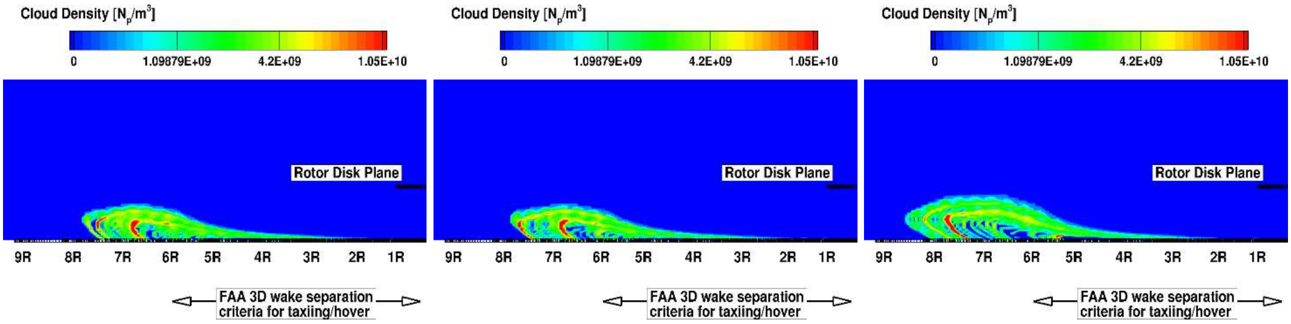

(d) Cloud density, h/R=1.0, Light scale helicopter (e) Cloud density, h/R=1.0, Medium scale helicopter (f) Cloud density, h/R=1.0, Heavy scale helicopter

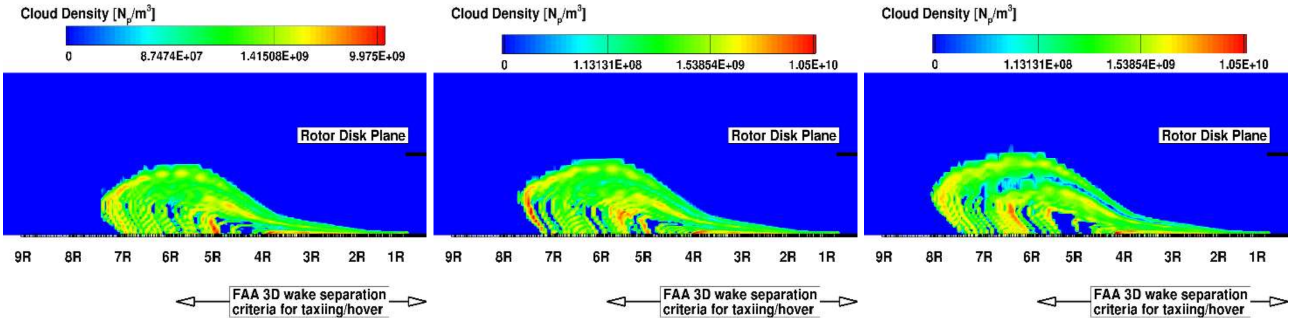

(g) Cloud density, h/R=1.5, Light scale helicopter (h) Cloud density, h/R=1.5, Medium scale helicopter (i) Cloud density, h/R=1.5, Heavy scale helicopter

Figure 3: Cloud Density [N_p/m^3] results for rotor at different heights above the ground and different scaling factors. All operational conditions of the small scaled rotor are listed in tab 3.